Morlet-wave-based modal identification in the time domain

I. Tomac[a,b,*], J. Slavič[a,**]

[a] *University of Ljubljana, Faculty of Mechanical Engineering, Aškerčeva cesta 6, SI-1000 Ljubljana, Slovenia*

[b] *University of Split, Faculty of Electrical Engineering, Mechanical Engineering and Naval Architecture, Ruđera Boškovića 32, HR-21000 Split, Croatia*

Cite as:

Ivan Tomac, Janko Slavič; Morlet-wave-based modal identification in the time domain, Mechanical Systems and Signal Processing, Volume 192, 1 June 2023, 110243

DOI: 10.1016/j.ymssp.2023.110243

Abstract

This research focuses on the time-domain identification of modal parameters using impact response excitation from signals with a relatively small dynamic range and high noise contamination (e.g., from high-speed cameras). The information required to identify the modal parameters is limited and is contained mostly at the beginning of the signal. In order to perform an identification from such a response, the following challenges have to be overcome: a good frequency-domain separation (for close modes), a good localisation in the time domain and an over-determination (to reduce uncertainty). To overcome these challenges this research introduces the Morlet-wave modal identification method as an extension of the Morlet-wave damping identification method, which has already proven capable of identifying the damping of short signals. Here, the method is extended to the modal parameters and an over-determination approach is proposed to reduce the uncertainty. The method identifies each mode shape separately from 10 to a maximum of 400 oscillations and at damping levels from 0.02% to 2% with a strong presence of noise in the signal. The method is tested on an experimental example and the results are compared to the classical modal identification methodology.

Keywords: Morlet-wave, modal identification, modal parameters, over-determination, noise

1. Introduction

Modal analysis is a standard tool in structural engineering practice [1]. The identification of the modal parameters mainly depends on the quality of the signals that are

*Corresponding author

**Principal corresponding author

Email addresses: itomac@fesb.hr (I. Tomac), janko.slavic@fs.uni-lj.si (J. Slavič)

acquired from the oscillating structure. Recently, new measurement techniques have been researched, such as high-speed cameras [2] or 3D printed sensors [3–5], which provide a relatively low dynamic range and are heavily contaminated with noise [6, 7]. Additionally, a higher frequency content is especially problematic when using impact excitation, because the measured displacement dies out quickly in the noise [8].

Recently, several authors have tackled the problem of modal identification using high-speed cameras and developed methods that utilize the over determination provided by dense spatial measurements [8–13]. Yang et al. [9] developed a technique based on blind source separation to perform the mode separation and identification of mode shapes, and damping was identified using the logarithmic decrement method [14]. Huňady and Hagara [10] introduced a method based on weighted frequency-response functions using the singular value decomposition to identify the mode shapes. The Rational Fraction Polynomial [15] and Frequency-Domain Polynomial [16] methods were used to identify the damping ratios and natural frequencies. Javh et al. [8] introduced the hybrid concept for experimental modal analysis by identifying system poles with a high dynamic-range sensor using the Least-Squares Complex-Frequency method [17] and the mode-shapes were identified from high-speed camera measurements using the Least-Squares Frequency-Domain method [18]. Li et al. [11] introduced the adaptive spatial filtering approach to extract and enhance the modal displacements' identification directly from pixels: mode-shapes were identified using the optimization approach by fitting sinusoid-based piecewise functions; natural frequencies and damping ratios were identified using the least-squares rational function method [19]. Wang et al. [12] presented the optimization approach of fitting the SDOF response on the measured data to obtain all the modal parameters from the under sampled response data. Willems et al. [13] presented the optimization procedure to match the mathematical model of the know system onto the underlying dynamics of the observed system, which is obtained from a dense measurement set by applying proper orthogonal mode decomposition.

The continuous wavelet transform [20] (CWT) can be used for analysing responses from low-dynamic-range sources, because it has a good time-and frequency-localization capability and it is resistant to noise [21]. With an application to real data, Staszewski [22] introduced three techniques to identify the damping from a MDOF impulse response with close modes, which were further researched by Slavič et al. [23] on the influence of edge-effect and frequency bandwidth using the Gabor wavelet. Chen et al. [24] performed an analytical study of the CWT based on the Morlet wavelet for the identification of damping and natural frequencies to provide general guidance for choosing wavelet-function parameters. Modal identification using the CWT was performed by several researchers: Le and Argoul [25] introduced the Cauchy wavelet on a free response and later it was used on responses with non-proportional damping by Erlicher and Argoul [26]. Modal identification was also performed on ambient responses by Lardies and Gouttebroze [27] using the modified Morlet wavelet. Le and Paultre [28] extended the CWT with singular value decomposition to detect modes under the noisy ambient responses. Le [29] performed a direct identification of the system poles from frequency-scale signal decomposition on ambient responses. Wang et al. [30] proposed to express the CWT of the free response signal as a weighted sum of the analytical signal components by relating the weight functions to the parameters of the

Gabor wavelet function. In this way, they were able to develop four different approaches to identify modal parameters, focusing on short signals and closely spaced modes. The CWT is exposed to the edge effect [31] and is computationally demanding [32]. The Morlet-wave-damping identification (MWDI) method was developed by Slavič and Boltežar [32] as an alternative to the CWT, which contains all the benefits from CWT, but does not suffer from the edge-effect and is computationally significantly less demanding. Theoretically, MWDI should be even more resistant to noise then the CWT, but the identification of the damping ratio is sensitive to the methods parameters [33] and the method does not identify the modal amplitude and the phase angle.

This manuscript researches an extension of the MWDI method [32] for amplitude and phase identification and proposes a least-squares approach to make the identification resistant to parameter selection. With the introduced method the identification procedure is simplified and the noisy measurements with the low dynamic can be evaluated for the modal parameters on relatively short signals.

The manuscript is organised as follows. In Sec. 2 the theoretical background is provided to support the development of the Morlet-wave modal method, which is presented in Sec. 3. The modal identification is tested in Sec. 4 on the numerically synthesised test cases with high levels of noise and the damping identification is compared to the eMWDI method. In Sec. 5 the modal identification is performed on the laboratory test case and the results of the identification were compared to the classical methods.

2. Theoretical background

2.1. Definition of mechanical systems

The development of a methodology for modal identification is based on the damped free response of a single-degree-of-freedom (SDOF) mechanical system that is defined as:

$$f_{\mathrm{m}}(t) = X e^{-\delta\,\omega_{\mathrm{n}}\,t} \cos\left(\omega_{\mathrm{d}}\,t - \phi\right) \tag{1}$$

where X and ϕ are the amplitude and phase angle that depend on the initial conditions, δ is damping ratio of the equivalent viscous damping, ω_{n} is the undamped natural frequency and ω_{d} is the damped natural frequency ($\omega_{\mathrm{d}} = \omega_{\mathrm{n}}\sqrt{1-\delta^2}$). The response from Eq. (1) can be extended to multi-degree-of-freedom (MDOF) mechanical systems as a sum of multiple SDOF responses if the proportional damping model [34] is assumed. Such a representation is also applicable to continuous systems [1].

2.2. Morlet wave integral

The Morlet wave integral was first introduced in the Morlet-wave damping identification method [32]. In this article the Morlet wave will be extended to the identification of modal parameters. The Morlet wave integral is based on the continuous wavelet transform (CWT) [20] with the application of the Morlet basic wavelet function [35]:

$$\tilde{I} = \int_0^T f_{\mathrm{m}}(t)\,\psi^*(t)\,\mathrm{d}t \tag{2}$$

where T is the length of the observed signal $f_{\mathrm{m}}(t)$, $\psi(t)$ is the basic wavelet function and * is a complex conjugate. The time T is defined as:

$$T = \frac{2\,\pi\,k}{\omega} \tag{3}$$

where k is the number of oscillations at the selected frequency ω. To reduce leakage in the frequency domain, k is limited to the positive integers. The Morlet wavelet function $\psi(t)$ is symmetrical around $T/2$ and it is defined as:

$$\psi_{\mathrm{n,\,k},\,\omega}(t) = (2\pi)^{-\frac{3}{4}} \sqrt{\frac{n\,\omega}{k}}\; e^{-\frac{n^2}{16\,k^2\,\pi^2}(k\,\pi-\omega\,t)^2} e^{i(k\,\pi-\omega\,t)} \tag{4}$$

where the parameter n sets the width of the Gaussian window function and controls the time/frequency spread. An important property of the continuous wavelet transform $\mathcal{W}\{\cdot\}$ (theoretical basic for the MWDI method) is the linearity, which makes it possible to separately analyse signals with multiple harmonic components:

$$\mathcal{W}_{\mathrm{n,\,k}_i,\,\omega_i}\left\{\sum_{i=1}^{N} a_i\, f_{\mathrm{m},i}\right\} = a_i \sum_{i=1}^{N} \mathcal{W}_{\mathrm{n,\,k}_i,\,\omega_i}\left\{f_{\mathrm{m},i}\right\} \tag{5}$$

where a is a constant, the index i denotes the frequency component and $k_i = T\,\omega_i/(2\pi)$. As will be discussed later, care should be taken in the parameters' selection for the wavelet function to achieve the appropriate frequency separation [20, 32].

2.3. The Morlet-wave-damping-identification method

Damping identification with the Morlet-wave is based on deriving analytical equations of the MW integral from the free response of the SDOF system (1). The base analytical expression is derived by inserting Eq. (1) into Eq. (2) and by setting the frequency of the Morlet wave (4) to the damped natural frequency of the system $\omega = \omega_{\mathrm{d}}$. The analytical expression of the Morlet-wave integral is obtained as follows:

$$I\,(n,\,k,\,\omega_{\mathrm{d}}) \approx X\left(\frac{\pi}{2}\right)^{\frac{3}{4}} \sqrt{\frac{k}{n\,\omega_{\mathrm{d}}}}\; e^{\frac{4\,\pi^2\,k^2\,\delta^2}{n^2(1-\delta^2)} - \frac{\pi\,\delta\,k}{\sqrt{1-\delta^2}}}\; e^{i(\pi\,k-\phi)}\; \varepsilon\,(n,\,k,\,\delta) \tag{6}$$

where $\varepsilon\,(n,\,k,\,\delta)$ is defined as:

$$\varepsilon\,(n,\,k,\,\delta) = \mathrm{erf}\left(\frac{n}{4} - \frac{2\,k\,\pi\,\delta}{n\sqrt{1-\delta^2}}\right) + \mathrm{erf}\left(\frac{n}{4} + \frac{2\,k\,\pi\,\delta}{n\sqrt{1-\delta^2}}\right) \tag{7}$$

The approximation in Eq. (6) is valid if the following condition is satisfied (for details see [32]):

$$k \leq \underbrace{\frac{n^2}{8\,\pi\,\delta}\sqrt{1-\delta^2}}_{k_{\mathrm{lim}}} \tag{8}$$

Based on Eq. (6) the information about damping is located in the absolute value of the Morlet-wave integral, with the natural frequency ω_d and the amplitude X, which are unknown. While ω_d can be identified relatively easy, the amplitude X can be cancelled out by obtaining the ratio between two MW integrals with different time-spread parameters n_1, n_2 [32]:

$$M(n_1,\, n_2,\, k,\, \delta) = \frac{|I(n_1,\, k,\, \omega_\mathrm{d})|}{|I(n_2,\, k,\, \omega_\mathrm{d})|} = e^{\frac{4\,\pi^2\,k^2\,\delta^2}{1-\delta^2}\,\frac{n_2^2-n_1^2}{n_1^2\,n_2^2}} \sqrt{\frac{n_2}{n_1}}\,\frac{\varepsilon\,(n_1,\, k,\, \delta)}{\varepsilon\,(n_2,\, k,\, \delta)} \tag{9}$$

M is theoretically derived and depends on the unknown damping ratio δ and the selected parameters of the Morlet-wave functions, where $n_1 > n_2$. The same ratio can be obtained from the measured data $f_\mathrm{m}(t)$ by numerically integrating Eq. (4), using the same selected parameters:

$$\tilde{M}\,(n_1,\, n_2,\, k,\, \omega_\mathrm{d}) = \frac{\left|\tilde{I}(n_1,\, k,\, \omega_\mathrm{d})\right|}{\left|\tilde{I}(n_2,\, k,\, \omega_\mathrm{d})\right|} \tag{10}$$

Finally, the damping is identified by solving the equation:

$$\tilde{M}\,(n_1,\, n_2,\, k,\, \omega_\mathrm{d}) - M\,(n_1,\, n_2,\, k,\, \delta) = 0 \tag{11}$$

for the unknown δ [32, 36].

2.4. Closely spaced modes

When the response of the system has closely spaced modes it is important to take care of the Morlet-wavelet function frequency spread defined as [32]:

$$\sigma_{\hat{\psi},i} = \frac{n\,\omega_i}{4\,\pi\,k} \tag{12}$$

The ratio $\tilde{M}$ in Eq. (10) is calculated with different time-spread parameters of the wavelet function n_1, n_2 and the parameter k, which regulate the frequency spread [20]. The frequency spread for the Morlet-wave function is defined in Eq. (12) and since $n_1 < n_2$, closely spaced frequencies ω_i and $\omega_{i\pm1}$ need to comply with [32]:

$$\max\left\{\frac{n_2\,\omega_i}{4\,\pi\,k},\, \frac{n_2\,\omega_{i\pm1}}{4\,\pi\,k}\right\} < |\omega_i - \omega_{i\pm1}| \tag{13}$$

3. Modal identification

Here, the idea of how to perform the modal identification with the Morlet wave is introduced. The Morlet wave was previously used to identify the damping [32] and the natural frequencies [33, 36]. However, here the identification of the damping and the exact natural frequency will be further enhanced and the identification of the amplitude and the phase will be introduced.

3.1. Exact natural frequency identification

The initial natural frequencies are estimated from the amplitude spectra of the response, such as picking the peaks. In the CWT, as well as the Morlet-wave method, the selected parameters n_1, n_2 and k can slightly shift the identified natural frequency [23]; therefore, for the identification of the damping ratio and amplitude of the oscillation need to be identified using the same selected parameters. The exact natural frequency is identified around the initial natural frequency $\tilde{\omega}_{\mathrm{d},i}$, by finding the maximum of the absolute value of the Morlet-wave integral (2):

$$\left.\frac{\partial \left|\tilde{I}\,(n,\,k,\,\omega\,)\right|}{\partial \omega}\right|_{\tilde{\omega}_{\mathrm{d},i}-\sigma_{\hat{\psi},i}}^{\tilde{\omega}_{\mathrm{d},i}+\sigma_{\hat{\psi},i}} = 0, \tag{14}$$

where $\sigma_{\hat{\psi},i}$ is the frequency spread of the Morlet-wave function defined with Eq (12).

3.2. Damping identification

Tomac et al. [33] found that the damping identified using the Eq. (11) was sensitive to the parameter k. The MWDI method tries to identify the damping on short signals, using as small a k as possible; however, as the k value decreases, the uncertainty in the identified result increases. Another problem when selecting k is related to the very small damping (e.g., $\delta = 0.02\,\%$), when a higher k is required to increase the sensitivity of the identification [32].

The identification of damping is based on Eq. (9) $M(n_1,\, n_2,\, k,\, \delta)$, which is an exponential function with k^2. As an example, the numerically synthesised data with noise were used to obtain a (numerical) experiment-based $\tilde{M}$ (10) (details in Sec. 4.1) and is shown for different k values in Fig. 1. Using these data the damping ratio δ can be identified from the least squares problem for multiple k values, where the cost function is:

$$F_{\mathrm{cost}}(\delta) = M(n_1,\, n_2,\, k,\, \delta) - \tilde{M}(n_1,\, n_2,\, k,\, \omega_{\mathrm{d}}) \tag{15}$$

The result of the minimization can be seen in Fig. 1 where the theoretical M (9) is plotted against the k values using the identified damping ratio.

An identification performed in this way decreased the uncertainty of the identified result (details in Sec. 4). This is because the identification no longer depends on the selection of a specific k value, instead it is performed using a range of k values.

3.3. Identification of amplitude and phase

After the identification of the natural frequency and the damping ratio, the amplitude and the phase angle can be identified. The procedure for the identification of the amplitude and the phase angle is similar to the identification of the damping ratio (15), only here it is based on the Morlet-wave integral I (6). The result of the Morlet-wave integral is complex valued and therefore the absolute value and the phase angle, which is derived from the

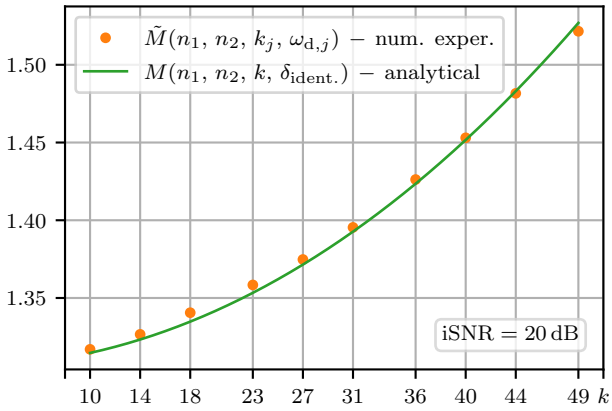

Figure 1: Analytical ratio M based on identified damping ratio and the ratio $\tilde{M}$ based on noisy synthetic signal versus k values ($n_1 = 5$, $n_2 = 10$).

argument, are minimised separately using the following cost functions:

$$F_{\mathrm{cost}}(X) = \left| I(n_1,\, k,\, \omega_{\mathrm{d}},\, \delta,\, X) \right| - \left| \tilde{I}\,(n_1,\, k,\, \omega_{\mathrm{d}}) \right| \tag{16}$$

$$F_{\mathrm{cost}}(\phi) = \phi - \tilde{\phi}(k) = \phi + \arctan\left(\frac{\Im\left[(-1)^k\, \tilde{I}\,(n_1,\, k,\, \omega_{\mathrm{d}}) \right]}{\Re\left[(-1)^k\, \tilde{I}\,(n_1,\, k,\, \omega_{\mathrm{d}}) \right]} \right) \tag{17}$$

3.4. Selection of default parameters

In this section the influence of the Morlet-wave parameters on the identification of the modal parameters will be discussed. Modal identification using the Morlet wave requires three parameters to be selected: n_1, n_2 and k. These parameters influence the sensitivity of the method. The choice of $n_{1,2}$ parameters has a twofold influence. One is on the theoretical M in Eq. (9), which is related to the damping ratio. Another influence is on the measurement-based $\tilde{M}$ in Eq. (10), which is related to the character of the signal in terms of noise and frequency separation which is important in close modes (13). The parameter n_1 should be set as low as possible to achieve a high sensitivity, but n_1 also influences the k_{lim} (8). With regards to [32], $n_1 = 5$ is a good balance between the sensitivity and the number of oscillations included in the analysis. The parameter n_2 should be at least double that of n_1 [32], and it is here set to $n_2 = 10$. To increase the sensitivity higher values could be used, but n_2 also influences the identification for closely spaced modes (13) and therefore high values should be avoided [32].

Parameter k defines the number of oscillations included in the analysis. In general we are interested in the shortest possible length that results in a successful identification. For a successful damping identification, it is reasonable that k is larger then 10 [32]; a higher k results in more data being included in the analysis, but for a free response, the instantaneous SnR [23] becomes low as the signal becomes smaller, while the noise is constant. Additionally, a high k value is limited by the assumptions made for the Morlet-wave [32], which is especially important at relatively high damping. This research will focus on a damping ratio below

2 %; using $\delta = 2\,\%$ and $n_1 = 5$, Eq. (8) results in $k_{\mathrm{lim}} = 49$. With smaller damping k_{lim} increases as defined in Eq. (8) and at $\delta \approx 0.25\,\%$ reaches 400, which will be the upper limit used here. In this research k will be in the range $10 \leq k \leq k_{\mathrm{lim}}$, for example, for $k_{\mathrm{lim}} = 400$ theoretically $400 - 10 = 390$ different values could be used; such a high over determination is not required and here only $N_{\mathrm{k}} = 10$ equally spaced integer values are used. For $k_{\mathrm{lim}} = 400$ this results in: $k_j = \big[10,\, 53,\, 96,\, 140,\, 183,\, 226,\, 270,\, 313,\, 356,\, 400\big]$. Similarly, if higher damping is estimated, k_{lim} would be smaller.

The parameters $n_{1,2}$ used in this study are tuned for high sensitivity, which is achieved at damping ratio of 0.25 % and $k_{\mathrm{lim}} = 400$. If one increases the damping ratio up to 2 %, k_{lim} decreases, allowing the method to work with high sensitivity, since M can always reach the maximum values. However, when the damping ratio decreases to 0.02 %, the sensitivity of the method decreases because k is fixed at 400 oscillations. For borderline cases, the problem is similar due to the signal errors having a large influence on the damping ratio, but the introduced overdetermination also reduces the influence of the signal errors on the identified damping ratio without having to change the parameters $n_{1,2}$. If the method is to be used beyond the recommended damping range, for higher damping ratios it should be necessary to reduce the sensitivity by increasing the n_1 parameter; and for extremely low damping ratios, the inclusion of more signal oscillations should be considered in addition to increasing the n_2 parameters. In the case of the closely spaced modes, the n_2 parameter can be reduced at the expense of sensitivity and/or by increasing the k_{lo} value according to Eq. (13) [32].

3.5. Modal identification algorithm

The algorithm for the identification is based on the following parameters, which are set as a default: $k_{\mathrm{lo}} = 10$, $k_{\mathrm{hi}} = k_{\mathrm{lim}}$, $N_{\mathrm{k}} = 10$, $n_1 = 5$ and $n_2 = 10$. For each mode at the initial $\tilde{\omega}_{\mathrm{d}}$, the modal parameters are identified in the following steps:

1) Select estimated damping ratio, obtain k_{lim} and k_j.
2) Identify exact natural frequency ω_{d} (Sec. 3.1).
3) Identify damping ratio δ (Sec. 3.2).
4) Identify amplitude X and phase angle ϕ (Sec. 3.3).

Step 1 starts with the estimated damping ratio that is used to define the initial k_{lim} value from Eq. (8). Then, the N_{k} integer k values are equally distributed from k_{lo} to $k_{\mathrm{hi}} = k_{\mathrm{lim}}$.

In step 2 the natural frequencies are identified for each k_j value in the range, by numerically searching for the maximum of the MW integral (14) (using $n = n_1$). A single natural frequency value ω_{d} is generated as a k-weighted average of the identified frequencies from the range $\omega_{\mathrm{d},j}$:

$$\omega_{\mathrm{d}} = \frac{1}{\sum_{j=1}^{N_{\mathrm{k}}} k_j} \sum_{j=1}^{N_{\mathrm{k}}} k_j\, \omega_{\mathrm{d},j} \tag{18}$$

In step 3 using $\omega_{\mathrm{d},j}$ the damping ratio δ is identified using the least-squares minimization of the cost function in Eq. (15). Here, the identified damping ratio needs to be checked

against the estimated; the identified damping ratio needs to be smaller then the estimated, otherwise the identification needs to restart at step 1 with a higher estimated damping ratio.

In step 4 using $\omega_{\mathrm{d},j}$ and δ (from step 2) the least-squares minimization of the cost functions in Eqs. (16) and (17) is performed to obtain the amplitude and the phase angle of the selected mode.

During the initial identification phase, the estimated damping should be correlated to the signal length, which will be used for the identification of the modal parameters. For instance, if the highest damping ratio of 2 % is selected, that would result in $k_{\mathrm{lim}} = 49$ (8), which means that up to 49 oscillations at the selected mode would be required for the identification. The algorithm for the method introduced in this research is implemented as an open-source Python package Morlet-Wave Modal [37].

In this article the presentation of the method is focused into the SISO test. While the extension to the SIMO test is straightforward, the extension to the MIMO tests would require significant further theoretical, numerical and experimental research (*e.g.* on mode participation factors and cross-coherence).

4. Numeric experiment

With synthetic experiments the identification of the modal parameters will be demonstrated; additionally, damping identification will be compared against the extended Morlet-wave damping-identification method (eMWDI) [33, 36], which is implemented as a Python package extended-mwdi [38]. The eMWDI method was presented in 2017 by Tomac et al. [33] and it is focused on damping identification, only. The introduced method identifies all modal parameters. Additionally, the damping identification is performed by simplified optimization approach, which resulted in damping identification from shorter signals.

4.1. Identification of modal parameters

The identification will be demonstrated on the free response of the SDOF system, generated with Eq. (1) by setting the parameters as follows: $\omega_{\mathrm{d}} = 100 \cdot 2\pi\ \mathrm{s}^{-1}$, $\delta = 1\,\%$, $X = 1$, $\phi = 0.7$. The response is sampled with 5000 Hz, the length of the signal is set to $T = 1$ s and it is contaminated using Gaussian noise with 0.1 variance, which resulted in iSNR = 0 dB [23] for 12 oscillations, see Fig. 2.

Step 1 – Initialization. The estimated damping ratio of 2 % is selected, resulting in $k_{\mathrm{lim}} = 49$ and k_j values are equally distributed between 10 and 49 that are given in Tab. 1.

Step 2 – Identification of natural frequency. The estimated natural frequency was set to $\tilde{\omega}_{\mathrm{d}} = 100.5 \cdot 2\pi\ \mathrm{s}^{-1}$. The results of identification per k_j value are shown in Tab. 1. The

Table 1: Identification of natural frequencies performed with step 2 in distributed k_j range.

k_j:	10	14	18	23	27	31	36	40	44	49
$f_{\mathrm{d},j}$ (Hz):	99.6	99.8	100.0	100.1	100.1	100.1	100.1	100.0	100.0	100.0

k-weighted average (18) is: $f_{\mathrm{d,\,identified}} = 100.0$ Hz.

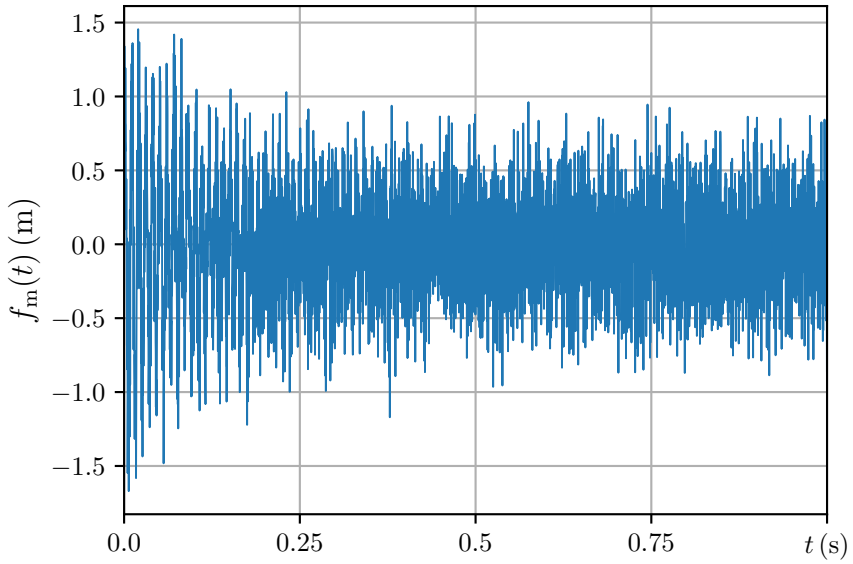

Figure 2: Free response of SDOF system used to demonstrate the modal parameter identification.

Step 3 – Identification of damping ratio. Damping is identified with the LS minimization of Eq. (15), using the exact natural frequencies $\omega_{\mathrm{d},j}$ to obtain $\tilde{M}(k_j)$ (10). The result of the minimization is $\delta_{\mathrm{identified}} = 0.9597\,\%$, which represents the identified damping ratio. To show how the theoretical M (9) fits $\tilde{M}(k_j)$, it is plotted against k, using the identified damping ratio, and it is depicted in Fig. 3. If the estimated damping was set to 1 %, then

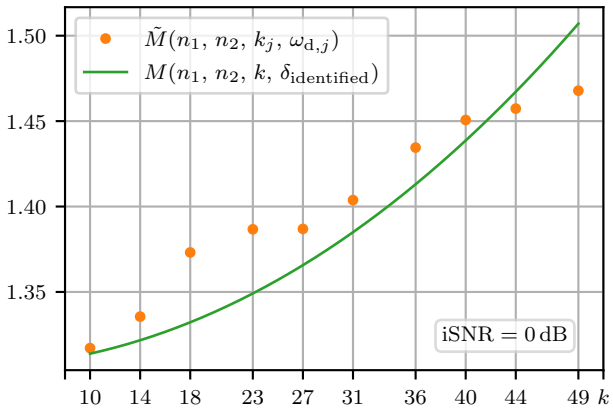

Figure 3: Theoretical ratio M based on identified damping as result of least-squares minimization with numerical experiment $\tilde{M}(k_j)$

a higher $k_{\mathrm{lim}} = 99$ would be available and the damping would be identified at 0.9712 %. It is important to point out that 0 dB is a very noisy signal and if the noise level was iSNR = 20 dB, damping would be identified at 1.00 % (for damping estimated at 2 %) as can be seen in Fig 1.

Step 4 – Identification of amplitude and phase angle. Using the identified damping, least-squares minimization of Eqs. (16) and (17) is performed and the following results are obtained: amplitude $X_{\text{identified}} = 0.98$ and phase $\phi_{\text{identified}} = 0.71$. The theoretical absolute value of the MW integral generated using the identified modal parameters $|I|$ (6), against k values is compared to the numerically synthesised $|\tilde{I}(k_j)|$ (2), which is shown in Fig. 4a. Like for the amplitude it is shown in Fig. 4b for the phase angle. If the noise level was reduced to iSNR = 20 dB then the identified amplitude would be 1.00 and the phase 0.71.

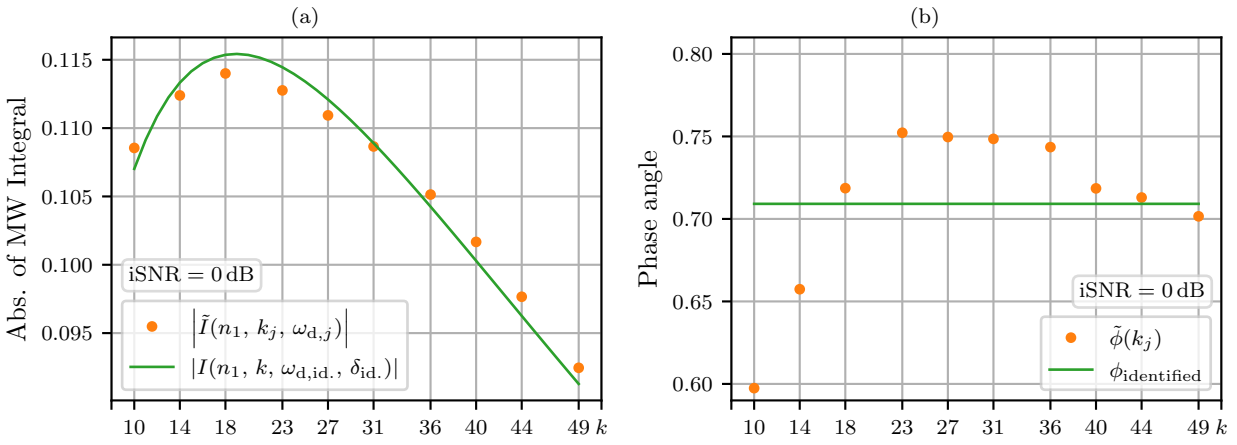

Figure 4: Comparison between MW integral I generated using the identified modal parameters and MW integral based on numerical experiment $\tilde{I}(k_j)$ for: (a) the absolute value and (b) the phase angle derived from the argument of the MW integral.

4.2. Comparison to extended Morlet-wave damping identification method

The comparison is performed on the synthesized response of the SDOF mechanical system contaminated with errors from the noise. The response is generated using the expression defined with Eq. (1) using the parameters $X = 1$, $\omega_{\text{d}} = 100 \cdot 2\pi$ s^{-1} and the phase is randomized for each run using a discrete uniform distribution [39] in the range: $-180° \leq \phi \leq 180°$. The methods are tested on three damping levels, which are given in Tab. 2. The signals are sampled with 5000 Hz and the length is set to $T = 4$ s. Both methods are tested on the default parameter set established in Sec. 3.5 and the k_{lim} is determined for each estimated damping ratio (see Tab. 2). All the responses are contaminated using Gaussian noise on two levels, defined with 0.001 and 0.01 variances. The noise level is expressed with iSNR for the k_{lim} oscillations that correspond to 20 and 10 dB with respect to the noise variances, for each damping ratio.

The comparative results of the damping identification are shown in Fig. 5, which are expressed as a relative error from the theoretical values. The bars extend from the 0.25 quantile to the 0.75 quantile surrounding the median with lines that extend to span the full dataset.

From the comparative results in Fig. 5 we can see that the damping was accurately identified with both methods, having median values within ±1 % for the case shown in

Table 2: Parameters of the numerical experiment used in the comparison between the MWModal and eMWDI methods.

δ (%):	0.25	0.1	0.05
$\delta_{\text{estimated}}$ (%):	2	0.8	0.4
k_{lim}:	49	124	248

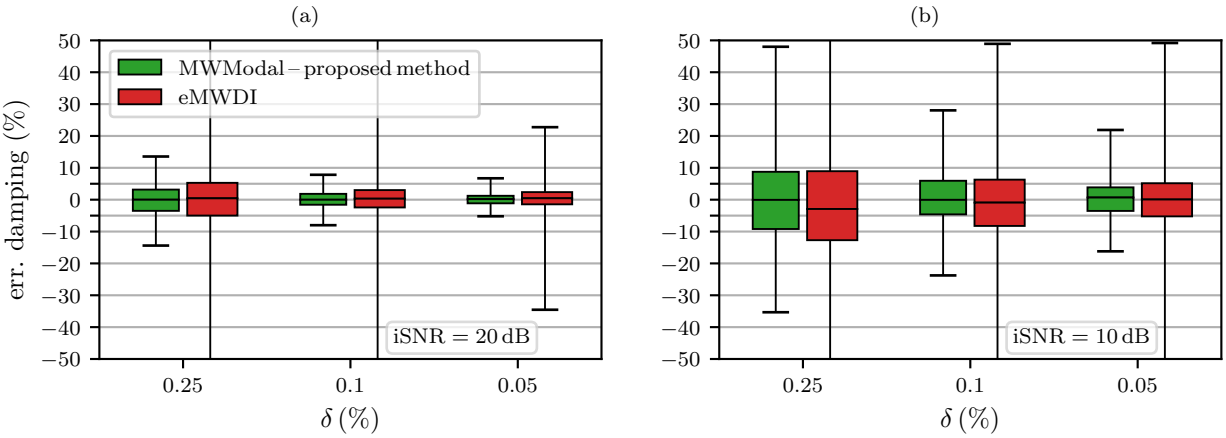

Figure 5: Comparative results of damping identification between two methods for different damping cases on the numerical experiment (400 samples each).

Fig. 5a. In the second case (Fig. 5b) the median error was slightly increased up to 3 % for eMWDI, while the MW modal remained below ±1 %. The improvement can be seen in a reduction of the first and fourth quantiles. In the case with iSNR = 20 dB for eMWDI they span from −90 to 50 % and in the case with iSNR = 10 dB, from −200 to 50 %. While for the MW modal at the worst case spans from −35 to 50 %, which proves the reduction of the uncertainty with the new method. The results could be improved if the lower damping ratios were estimated, which would lead to higher k_{lim} values and consequently the longer signal utilization. Additionally, the MW modal method performed the identification using just ten k values, while the eMWDI used all the k values from the selected range. The identification results for the natural frequencies using both methods span ±0.1 % and therefore the results are omitted from the text.

4.3. Amplitude and phase identification

The amplitude and phase are identified using only using the MW modal method as a continuation from Sec. 4.2. The amplitude results are shown in Fig. 6a, which are expressed as the relative error between the identified and the theoretical. The phase-angle results are shown in Fig. 6b, where they are expressed as the difference between the identified and the theoretical angle: $\Delta\phi = \phi_{\text{identified}} - \phi$.

The amplitude (Fig. 6a) was accurately identified in all cases, even though that higher noise level increased the error span, but still all samples were identified within ±0.15 %. It is

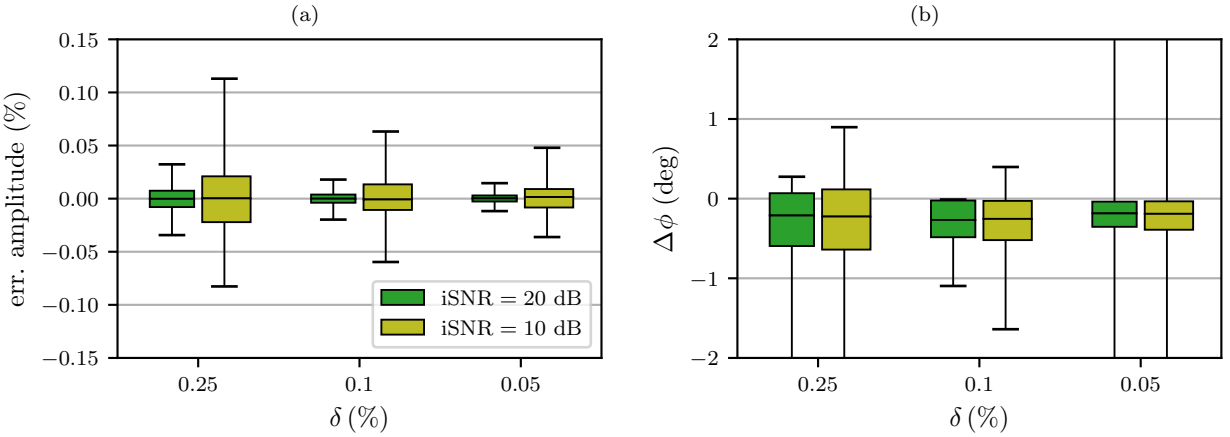

Figure 6: Identification results of numerical experiment using Morlet-wave modal method for (a) amplitude and (b) phase angle for different damping cases (400 samples each).

similar for the phase angle (Fig. 6b) the where difference in the identified phase-angle span was within $\pm 2°$, although for cases at damping ratios 0.25 and 0.05 % the first quantile spans from $-360°$ and in the second case the fourth quantile spans to $360°$. It is because the one sampled phase angle out of five that were near the boundary angles ($178° \leq |\phi| \leq 180°$) was identified with a different sign for the case at $\delta = 0.25\,\%$ and two out of nine at $\delta = 0.05\,\%$ case, for both noise levels equally. It can be observed that the identification of the amplitude and the phase performs well at applied noise levels.

5. Experimental testing

Modal identification is performed on the experimental data obtained from the laboratory test model of the freely supported steel beam ($w \times h \times d = 600 \times 12 \times 50$ mm). The identification is performed with the developed method using the Python package MW Modal [37]. For verification, the results are compared with the classical modal identification methods: Least-Squares Complex-Frequency method [17] for identification of natural frequencies and damping ratios and Least-Squares Frequency-Domain method [18] for identification of amplitudes and phase angles. These methods are implemented in the python package pyEMA [40] and work in the frequency domain with the frequency response functions (FRFs). However, the MW modal method is developed for the identification of modal parameters from the signals in the time domain. In order to adequately compare the identified amplitudes and phase angles, the MW modal method is exceptionally applied to the impulse response function (IRF), a time domain representation of the FRF.

The beam was excited with a modal hammer (PCB 086C03) at the same spot where the accelerometer (PCB T333B30) was placed, which is 420 mm from the left hand side of the beam. The experimental setup is show in Fig. 7. The response and the stimulus signals were sampled using the NI-9234 data-acquisition card with a sampling rate $f_\mathrm{S} = 51200$ Hz for 2 s. The impulse response function was used for the identification on the first six natural

frequencies $\tilde{f}_{\mathrm{d},i}$, which were picked from the FRF magnitude plot, and the values are shown in the second row of Tab. 3.

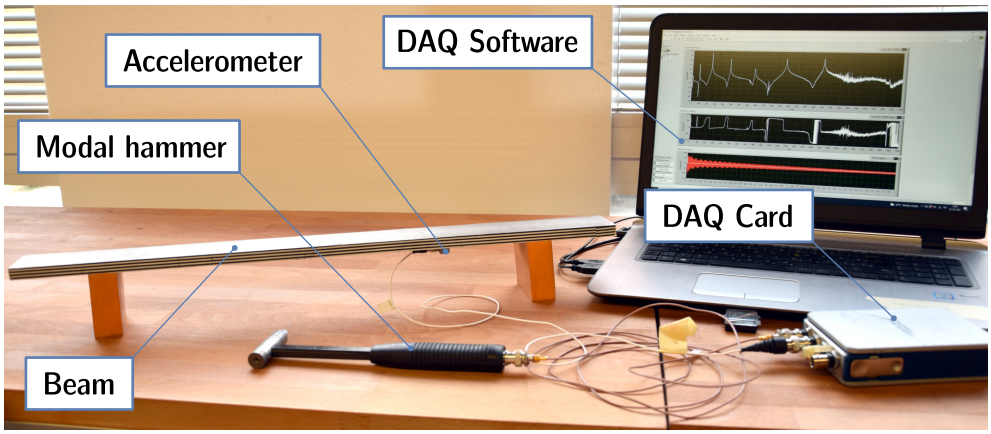

Figure 7: Experimental setup.

The identification is performed using the Morlet Wave Modal method on the IRF. The estimated damping for a freely supported steel beam was 0.1 % for all modes (step 1). Such a damping ratio resulted in a maximum k_{lim} value and because of relatively high natural frequencies the low k value was increased by setting the $k_{\mathrm{lo}} = 20$. The identification performed with pyEMA was realized on the FRF in the range between 100 and 4000 Hz. The results are shown in Tab. 3.

Table 3: Comparative results of modal parameter identification from experimental data.

	Mode:	1^{st}	2^{nd}	3^{rd}	4^{th}	5^{th}	6^{th}
	$\tilde{f}_{\mathrm{d}}$ (Hz):	175	481	942	1551	2306	3201
MW Modal	k_{lim}	348	400	400	400	400	400
	f_{d} (Hz):	175.1	481.1	941.8	1550.4	2306.0	3200.4
	δ (%):	0.097	0.021	0.055	0.213	0.142	0.103
	X ($\mathrm{m\,s^{-2}\,N^{-1}}$):	106	1717	1234	600	7576	8794
	ϕ (°):	−93.7	−90.4	−90.7	−74.2	−85.7	−85.9
pyEMA	f_{d} (Hz):	175.1	481.1	941.8	1550.8	2305.9	3201.3
	δ (%):	0.095	0.022	0.054	0.222	0.143	0.109
	X ($\mathrm{m\,s^{-2}\,N^{-1}}$):	110	1908	1216	614	7589	8979
	ϕ (°):	−81.9	−76.5	−87.9	−72.0	−86.7	−78.1

From the ratio $k_{\mathrm{lim}} \big/ \tilde{f}_{\mathrm{d}}$ (3) we can determine the signal length required to perform the identification, which is only 125ms for the 6^{th} mode. The pyEMA operated on the single FRF and the damping was identified with the relative error between methods below 5 %, except for the 6^{th} mode, where the error was slightly higher, i.e., 6 %. The time required to

perform modal identification using the introduced method (as implemented in MWModal package) was 1.1 s, while for traditional methods (LSCE/LSFD methods, as implemented in the pyEMA) required 2.3 s, on a laptop with the processor: 11$^{\text{th}}$ Gen Intel® Core™ i7-1185G7 @ 3.00GHz.

6. Conclusion

The Morlet-wave-based modal identification method is introduced. The theoretical background of which is described in detail, starting from previous research on the Morled-wave and the continuous-wavelet-transform-based damping identification. The method is tested numerically and experimentally. The numerical research of synthesized experimental data that is heavily contaminated with noise showed better results than the Morlet-Wave damping identification method. *e.g.*, a simulated impact response with instantaneous SNR = 0 dB was, for a very short signal (12 oscillations), 4 % away from the true value. A parametric comparison against the extended Morlet-Wave damping-identification method showed significantly lower uncertainty for the identified damping ratio.

An experimental validation was performed on the laboratory test case, as a steel beam excited by a hammer and the response was measured with an accelerometer. The identification results were compared to the classical modal identification methodologies in the frequency domain. The accuracy of all the modal parameters was comparable to the classical method, while the modal identification with the proposed method was performed for a fraction of the time-domain data, only. The experimental research confirmed that the modal parameters are successfully identified using impact excitation from relatively noisy data and relatively short signals.

Based on the numerical and theoretical research, this manuscript confirms that the proposed method is expected to be successful in the time-domain identification of modal parameters from relatively-short and low-dynamic range data, heavily contaminated with noise (*e.g.*, high-speed camera measurements, 3D-printed sensors).

Acknowledgement

The authors acknowledge partial financial support from the European Union's Horizon 2020 research and innovation programme under the Marie Skłodowska-Curie grant agreement No 101027829 and the Slovenian Research Agency (N2-0144, J2-3045).

References

[1] J. He, Z.-F. Fu, Modal Analysis, Butterworth-Heinemann, 2001. doi:10.1016/B978-0-7506-5079-3.X5000-1.

[2] J. Baqersad, P. Poozesh, C. Niezrecki, P. Avitabile, Photogrammetry and optical methods in structural dynamics – a review, Mechanical Systems and Signal Processing 86 (2017) 17–34. URL: https://doi.org/10.1016/j.ymssp.2016.02.011. doi:10.1016/j.ymssp.2016.02.011.

[3] V. Zega, M. Invernizzi, R. Bernasconi, F. Cuneo, G. Langfelder, L. Magagnin, M. Levi, A. Corigliano, The first 3d-printed and wet-metallized three-axis accelerometer with differential capacitive sensing, IEEE Sensors Journal 19 (2019) 9131–9138. doi:10.1109/JSEN.2019.2924473.

[4] M. Arh, J. Slavič, Single-process 3d-printed triaxial accelerometer, Advanced Materials Technologies 7 (2022) 2101321. doi:10.1002/admt.202101321.
[5] T. Košir, J. Slavič, Single-process fused filament fabrication 3d-printed high-sensitivity dynamic piezoelectric sensor, Additive Manufacturing 49 (2022) 102482. doi:10.1016/j.addma.2021.102482.
[6] T. Schmidt, J. Tyson, K. Galanulis, Full-field dynamic displacement and strain measurement using advanced 3d image correlation photogrammetry: part 1, Experimental Techniques 27 (2003) 47–50. doi:10.1111/j.1747-1567.2003.tb00115.x.
[7] R. Costantini, S. Susstrunk, Virtual sensor design, 2004, p. 408. doi:10.1117/12.525704.
[8] J. Javh, J. Slavič, M. Boltežar, High frequency modal identification on noisy high-speed camera data, Mechanical Systems and Signal Processing 98 (2018) 344–351. URL: https://linkinghub.elsevier.com/retrieve/pii/S0888327017302637. doi:10.1016/j.ymssp.2017.05.008.
[9] Y. Yang, C. Dorn, T. Mancini, Z. Talken, G. Kenyon, C. Farrar, D. Mascareñas, Blind identification of full-field vibration modes from video measurements with phase-based video motion magnification, Mechanical Systems and Signal Processing 85 (2017) 567–590. doi:10.1016/j.ymssp.2016.08.041.
[10] R. Huňady, M. Hagara, A new procedure of modal parameter estimation for high-speed digital image correlation, Mechanical Systems and Signal Processing 93 (2017) 66–79. URL: https://doi.org/10.1016/j.ymssp.2017.02.010. doi:10.1016/j.ymssp.2017.02.010.
[11] M. Li, G. Feng, R. Deng, F. Gao, F. Gu, A. D. Ball, Structural vibration mode identification from high-speed camera footages using an adaptive spatial filtering approach, Mechanical Systems and Signal Processing 166 (2022) 108422. URL: https://doi.org/10.1016/j.ymssp.2021.108422. doi:10.1016/j.ymssp.2021.108422.
[12] Y. Wang, F. S. Egner, T. Willems, M. Kirchner, W. Desmet, Camera-based experimental modal analysis with impact excitation: Reaching high frequencies thanks to one accelerometer and random sampling in time, Mechanical Systems and Signal Processing 170 (2022) 108879. URL: https://doi.org/10.1016/j.ymssp.2022.108879. doi:10.1016/j.ymssp.2022.108879.
[13] T. Willems, F. S. Egner, Y. Wang, M. Kirchner, W. Desmet, F. Naets, Time-domain model identification of structural dynamics from spatially dense 3d vision-based measurements, Mechanical Systems and Signal Processing 182 (2023) 109553. URL: https://doi.org/10.1016/j.ymssp.2022.109553. doi:10.1016/j.ymssp.2022.109553.
[14] W. T. Thomson, Theory of Vibration with Applications, volume 4, CRC Press, 1993. doi:10.1201/9780203718841.
[15] M. H. Richardson, D. L. Formenti, Parameter estimation from frequency response measurements using rational fraction polynomials, volume 1, 1982, pp. 167–186.
[16] R. Allemang, D. Brown, A unified matrix polynomial approach to modal identification, Journal of Sound and Vibration 211 (1998) 301–322. doi:10.1006/jsvi.1997.1321.
[17] P. Guillaume, P. Verboven, S. Vanlanduit, Frequency-domain maximum likelihood identification of modal parameters with confidence intervals, volume 1, 1998, pp. 359–366.
[18] H. V. D. Auweraer, W. Leurs, P. Mas, L. Hermans, Modal parameter estimation from inconsistent data sets, volume 4062, 2000.
[19] A. A. Ozdemir, S. Gumussoy, Transfer function estimation in system identification toolbox via vector fitting, IFAC-PapersOnLine 50 (2017) 6232–6237. doi:10.1016/j.ifacol.2017.08.1026.
[20] S. Mallat, A Wavelet Tour Of Signal Processing, 2nd ed., Academic Press, 1999.
[21] M. Ruzzene, A. Fasana, L. Garibaldi, B. Piombo, Natural frequencies and dampings identification using wavelet transform: application to real data, Mechanical systems and signal processing 11 (1997) 207–218. doi:10.1006/mssp.1996.0078.
[22] W. J. Staszewski, Identification of damping in mdof systems using time-scale decomposition, Journal of sound and vibration 203 (1997) 283–305. URL: https://doi.org/10.1006/jsvi.1996.0864. doi:10.1006/jsvi.1996.0864.
[23] J. Slavič, I. Simonovski, M. Boltežar, Damping identification using a continuous wavelet transform, application to real data, Journal of Sound and Vibration 262 (2003) 291–307. URL: https://doi.org/10.1016/S0022-460X(02)01032-5. doi:10.1016/S0022-460X(02)01032-5.

[24] S.-L. Chen, J.-J. Liu, H.-C. Lai, Wavelet analysis for identification of damping ratios and natural frequencies, Journal of Sound and Vibration 323 (2009) 130–147. doi:10.1016/j.jsv.2009.01.029.

[25] T.-P. Le, P. Argoul, Continuous wavelet transform for modal identification using free decay response, Journal of Sound and Vibration 277 (2004) 73–100. URL: https://www.sciencedirect.com/science/article/pii/S0022460X03012124. doi:10.1016/j.jsv.2003.08.049.

[26] S. Erlicher, P. Argoul, Modal identification of linear non-proportionally damped systems by wavelet transform, Mechanical Systems and Signal Processing 21 (2007) 1386–1421. URL: https://www.sciencedirect.com/science/article/pii/S0888327006000719. doi:10.1016/j.ymssp.2006.03.010.

[27] J. Lardies, S. Gouttebroze, Identification of modal parameters using the wavelet transform, International Journal of Mechanical Sciences 44 (2002) 2263–2283. URL: https://www.sciencedirect.com/science/article/pii/S0020740302001753. doi:10.1016/S0020-7403(02)00175-3.

[28] T.-P. Le, P. Paultre, Modal identification based on continuous wavelet transform and ambient excitation tests, Journal of Sound and Vibration 331 (2012) 2023–2037. URL: https://www.sciencedirect.com/science/article/pii/S0022460X12000600. doi:10.1016/j.jsv.2012.01.018.

[29] T.-P. Le, Use of the morlet mother wavelet in the frequency-scale domain decomposition technique for the modal identification of ambient vibration responses, Mechanical Systems and Signal Processing 95 (2017) 488–505. URL: https://doi.org/10.1016/j.ymssp.2017.03.045. doi:10.1016/j.ymssp.2017.03.045.

[30] S. Wang, W. Zhao, G. Zhang, H. Xu, Y. Du, Identification of structural parameters from free vibration data using gabor wavelet transform, Mechanical Systems and Signal Processing 147 (2021) 107122. doi:10.1016/J.YMSSP.2020.107122.

[31] T. Kijewski, A. Kareem, On the presence of end effects and their melioration in wavelet-based analysis, Journal of Sound and Vibration 256 (2002) 980–988. doi:10.1006/jsvi.2001.4227.

[32] J. Slavič, M. Boltežar, Damping identification with the morlet-wave, Mechanical Systems and Signal Processing 25 (2011) 1632–1645. URL: https://doi.org/10.1016/j.ymssp.2011.01.008. doi:10.1016/j.ymssp.2011.01.008.

[33] I. Tomac, Ž. Lozina, D. Sedlar, Extended morlet-wave damping identification method, International Journal of Mechanical Sciences 127 (2017). URL: https://doi.org/10.1016/j.ijmecsci.2017.01.013. doi:10.1016/j.ijmecsci.2017.01.013.

[34] J. W. S. Rayleigh, The Theory of Sound, 2nd ed., Dover publications, 1945.

[35] P. Goupillaud, A. Grossmann, J. Morlet, Cycle-octave and related transforms in seismic signal analysis, Geoexploration 23 (1984) 85 – 102. doi:10.1016/0016-7142(84)90025-5.

[36] I. Tomac, J. Slavič, Damping identification based on a high-speed camera, Mechanical Systems and Signal Processing 166 (2022) 108485. URL: https://linkinghub.elsevier.com/retrieve/pii/S0888327021008281. doi:10.1016/j.ymssp.2021.108485.

[37] I. Tomac, J. Slavič, ladisk/morletwavemodal: Mwmodal v0.5.1, 2022. URL: https://doi.org/10.5281/zenodo.7002905. doi:10.5281/zenodo.7002905.

[38] I. Tomac, J. Slavič, itomac/extended morlet-wave: emwdi v0.3.1, 2022. URL: https://doi.org/10.5281/zenodo.6979893. doi:10.5281/zenodo.6979893.

[39] D. Lemire, Fast random integer generation in an interval, ACM Trans. Model. Comput. Simul. 29 (2019). URL: https://doi.org/10.1145/3230636. doi:10.1145/3230636.

[40] K. Zaletelj, T. Bregar, D. Gorjup, J. Slavič, ladisk/pyema: Release of the version v0.24, 2020. URL: https://doi.org/10.5281/zenodo.4016671. doi:10.5281/zenodo.4016671.